Cell, Vol. 57, 493–502, May 5, 1989, Copyright © 1989 by Cell Press

Highly Localized Tracks of Specific Transcripts within Interphase Nuclei Visualized by In Situ Hybridization

Jeanne Bentley Lawrence, Robert H. Singer, and Lisa M. Marselle
Department of Cell Biology
University of Massachusetts Medical School
Worcester, Massachusetts 01655

Summary

Use of in situ hybridization optimized for fluorescent detection of nuclear RNA has revealed a striking localization of specific viral RNAs within nuclei of cells latently infected with EBV. Several hundred kb of specific transcripts is sharply restricted to a small region of the nucleus, frequently in a curvilinear "track." Detection of nuclear RNA was evidenced by hybridization without denaturation, sensitivity to RNAase, inhibition by actinomycin D, and specificity of transcribed sequences. Results indicate that RNA "tracks" extend from an internal genome into the nuclear periphery, and that RNA transport may be coupled to transcription. Localized nRNA is apparent for other viral sequences, different lymphoblastoid cell lines, nuclei prepared by two different methods, and an abundant, nonviral transfected sequence. Implications for understanding nuclear organization and the investigation of gene expression are discussed.

Introduction

The complex machineries responsible for the synthesis and processing of nuclear RNA are currently the focus of much investigation. The first product of eukaryotic gene expression is generally a high molecular weight nuclear RNA (nRNA) that undergoes a series of complex processing steps, including removal of intervening sequences, capping at the 5′ end, and polyadenylation at the 3′ end, to produce the smaller mature mRNA that is ultimately transported to the cytoplasm for translation. It is known that heterogeneous nuclear RNA (hnRNA) is heavily complexed with nuclear proteins to form the hnRNP particle (Pederson, 1974; Beyer et al, 1977; Pederson and Davis, 1980) and that discrete classes of small nuclear RNAs are active parts of the spliceosome responsible for intron removal (Lerner et al., 1980; reviewed in Sharp, 1987). While progress advances rapidly with regard to identifying the biochemical and molecular components of the transcriptional and processing machineries, there is as yet little conception of how these components are integrated into the dynamic structure of the nucleus. Basic questions such as whether active genes or their transcripts and the processing of such are specifically localized within the nucleus are unresolved. How transcripts are transported through the nucleoplasm to the nuclear pores is unknown (reviewed in Clawson et al., 1985; Agutter, 1985; Schroder et al., 1987).

A number of laboratories seeking to define the basic physical structure of the nucleus have provided evidence for a nonchromatin nuclear matrix composed of a network of predominantly proteinaceous fibrils (Georgiev and Chentsov, 1960; Berezny and Coffey, 1974; Brasch, 1982; Herman et al., 1978; Capco and Penman, 1983; Fey et al., 1984), with which hnRNA is intimately associated (Long et al., 1979; Jackson et al., 1981; Ross et al., 1982; van Eekelen et al., 1981; Berezney, 1980; Fey et al., 1986). It has been further indicated that nuclear RNA may contribute to the maintenance of nuclear structure (Fey et al., 1986). Based upon these and other considerations, it has been proposed (Blobel, 1985; Agutter, 1985; Schroder et al., 1987) that RNAs are unlikely to diffuse freely through the highly viscous nucleus, but are more likely to be actively transported from their site of synthesis to the nuclear pores across a "solid-phase" nuclear architecture.

The investigation of nuclear structure and its relationship to nuclear RNA metabolism would be greatly facilitated by a tool to visualize distribution of specific RNA sequences directly within the structural context of intact nuclei. Application of such a tool could provide immediate insights into the "solid-phase" versus the "free-diffusion" models of nuclear organization and RNA transport (Agutter, 1985). Further, the ability to visualize specific RNAs at their site of transcription would be generally valuable for the study of gene expression by providing a cytological assay for gene transcription directly within individual cells.

In the work presented here, we have developed and applied nonisotopic in situ hybridization procedures with the objective of providing direct visualization of specific primary transcripts within interphase nuclei. Previously described methods for fluorescence detection of single-copy genes (Lawrence et al., 1988a) have been adapted and extended for the localization of nuclear transcripts. In most experiments, transcripts synthesized from an integrated Epstein–Barr Virus (EBV) genome in a human lymphoma cell line were investigated. This latently infected cell line, Namalwa, contains two copies of the EBV genome closely integrated on chromosome 1 (Lawrence et al., 1988a), and does not contain episomal genomes (Henderson et al., 1983). The expression of the viral genome in these cells has been well characterized, and the line provides good experimental material with which to attempt visualization of specific nuclear RNAs since transcripts from specific regions of the viral genome accumulate within the nucleus (Hayward and Kieff, 1976; Powell et al., 1979; King et al., 1980; van Santen et al., 1983; Dambaugh et al., 1986; Austin et al., 1988).

Results

Biotin-labeled DNA probes representing specific fragments of the EBV genome were hybridized to interphase nuclei in cytogenetic preparations of Namalwa lymphoma cells, and hybridization was detected with fluorescein avidin. The primary probe utilized was a plasmid containing the BamHI W fragment (Bam W) of the EBV genome.

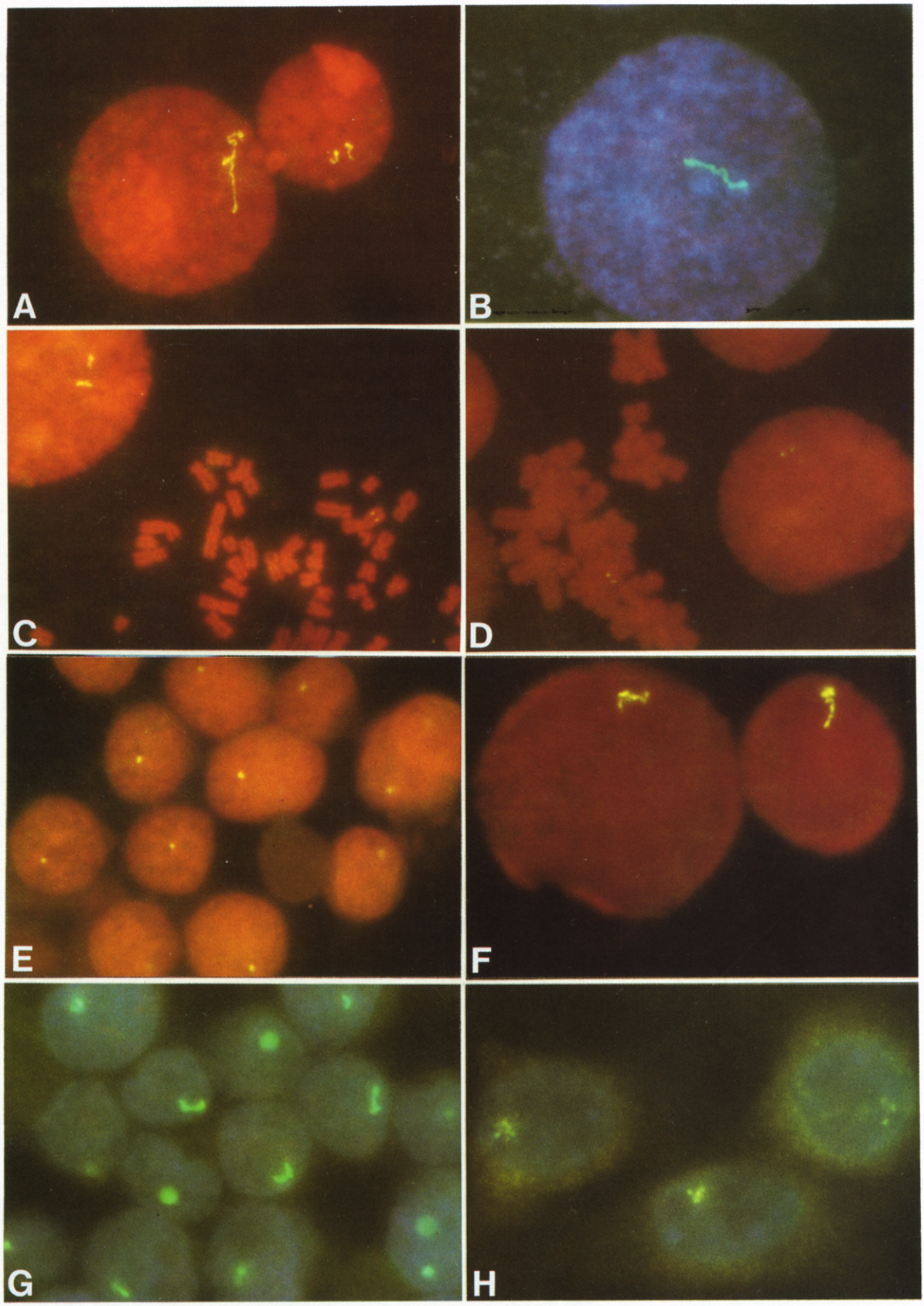
A
B
C
D
E
F
G
H

The Bam W region is a 3 kb sequence, tandemly repeated 6–10 times in the EBV genome, hence representing 18–30 kb of DNA (Henderson et al., 1983). Bam W sequences are well represented in nuclear RNA of Namalwa cells, and primary transcripts up to 20 kb long that contain these sequences are extensively spliced to form the 3 kb LT-1 mRNA, present in low levels in polyadenylated cytoplasmic RNA (van Santen et al., 1983; Dambaugh et al., 1986).

In initial experiments, previously described methodology for fluorescence detection of single-copy nuclear DNA (Lawrence et al., 1988a) was modified to allow direct visualization of specific nuclear RNAs. While methodological details will be confined to Experimental Procedures, it was found that omission of denaturation, heat treatment, and RNAase treatment, coupled with frozen storage of slides and careful selection and quality control of key reagents, promoted reproducible detection of nuclear RNA with the high resolution of fluorescence microscopy. Nonisotopic in situ hybridization with the EBV Bam W probe under the appropriate conditions revealed a striking localization of these RNA sequences within interphase nuclei. There was no evidence of a diffuse or broad regional distribution. On the contrary, the transcripts detected were highly restricted to a specific site in each nucleus, with accumulated transcripts forming a bright focus or curvilinear fluorescent structure, referred to as a "track". These formations were particularly dramatic in large decondensed nuclei, where they frequently extended across almost half of the nucleus (Figures 1A and 1B). No such structures were ever observed after hybridization with biotinated pBR322 probe.

Results using several different experimental strategies definitively support the conclusion that these structures represent detection of nuclear transcripts. In samples for which DNA had been denatured prior to hybridization, Bam W sequences are detected at the EBV integration site on metaphase chromosome 1, as well as in interphase nuclei (Figure 1C). However, if denaturation of double-stranded DNA is omitted prior to hybridization, there is no detectable hybridization to metaphase chromosomes (which do not transcribe RNA), but fluorescent "tracks" are still observed in interphase nuclei (Figures 1A and 1B). In nondenatured preparations, all nuclear signal is removed by treatment with RNAase H after hybridization (data not shown). In denatured preparations treated with RNAase H (Figures 1D and 2B), signal is reduced to just two closely paired spots in interphase nuclei, representing two closely integrated viral genomes, as previously described (Lawrence et al., 1988a). Cells were treated with actinomycin D prior to fixation in order to inhibit transcription, and were hybridized without prior denaturation of DNA. Fluorescent nuclear signals were diminished in size and intensity by a 1 hr incubation in actinomycin D and were essentially eliminated by a 5 hr incubation (see below). Finally, the degree to which different regions of the EBV genome are transcribed in Namalwa cells has been well characterized by conventional filter and solution hybridization techniques (reviewed in Dambaugh et al., 1986). We performed in situ hybridization with probes for four different fragments of the EBV genome, two of which are known to be heavily transcribed (BamHI fragments W and Y/H), one of which is transcribed at lower levels (BamHI K), and one which is not transcribed in this line (BamHI A). As illustrated in Figure 2, there was a good correlation between the in situ assay and conventional hybridization results. The most prominent RNA signals were observed for the W and Y/H probes (Figures 2A and 2C, respectively), fainter signals with the K probe (data not shown), and essentially no RNA signal using the A probe (Figure 2D).

Dimensions, Substructure, and Quantitation of RNA Content in Interphase Nuclei

The precise, elongated dimensions of the nuclear RNA signals were highly suggestive of a succession of nuclear RNA transcripts confined to a track. Approximately 90% of nuclei contained a single focus or "track" after hybridization for RNA, although it was not infrequent for nuclei to contain two, and occasionally more. It was evident from the dimensions and intensity of the RNA signals, relative to the DNA signals with the same probe, that many RNA molecules were being detected (compare Figures 1A, 1C, and 1D). As previously described (Lawrence et al., 1988a),

Figure 1. Fluorescent Detection of Specific RNA and DNA Sequences within Nuclei Stained Simultaneously for Total DNA

Biotinated probes were hybridized in situ, and specific hybridization was detected with fluorescein-avidin (yellow–green). Total DNA was stained with either propidium iodide (red) or DAPI (blue). (A)–(D) show hybridization to cytogenetic preparations of Namalwa cells.

(A) Track of EBV BamHI fragment W (Bam W) RNA within nondenatured interphase nuclei of Namalwa cells. Total magnification 1000×.

(B) Same as in (A), in DAPI-stained nuclei. Fluorescein-avidin fluorescence appears green. 1400×.

(C) Simultaneous hybridization to both viral RNA and DNA in denatured samples. Spots of yellow fluorescence on each sister chromatid of chromosome 1 indicate the localization of the integrated EBV genomes (see (D) below). Interphase nuclei show larger fluorescent signals, indicative of Bam W RNA. 1000×.

(D) Hybridization to Bam W DNA in denatured and RNAase H-treated samples. Signal in G1 interphase nuclei appears as two closely spaced fluorescent spots indicative of the two EBV genomes closely integrated on one homolog of chromosome 1. Due to increased chromatin condensation, on metaphase chromosomes the two fluorescent spots coalesce into one signal on each of the two sister chromatids. 1000×.

(E) Residual Bam W nuclear RNA in nuclei of intact Namalwa cells treated with actinomycin D for 3 hr prior to fixation in paraformaldehyde. Note that the tracks are much shorter (compare with (G)) and distribute within the internal region of the nucleus, not at the edge. 1500×.

(F) EBV Bam W RNA in nuclei from IB-4 cells. Note the large accumulation of RNA at the end of the track near the outer edge of the nucleus. 1000×.

(G) Same as in (A) and (B), except that hybridization was to Bam W RNA in nondenatured nuclei of paraformaldehyde-fixed intact Namalwa cells. 1500×.

(H) Hybridization to a *neu* oncogene (erb B2) RNA in intact 3T3 cells transfected with a plasmid containing the *neu* oncogene. Foci of nuclear RNA are apparent, and punctate staining throughout the cytoplasm indicates cytoplasmic mRNA. 1800×.

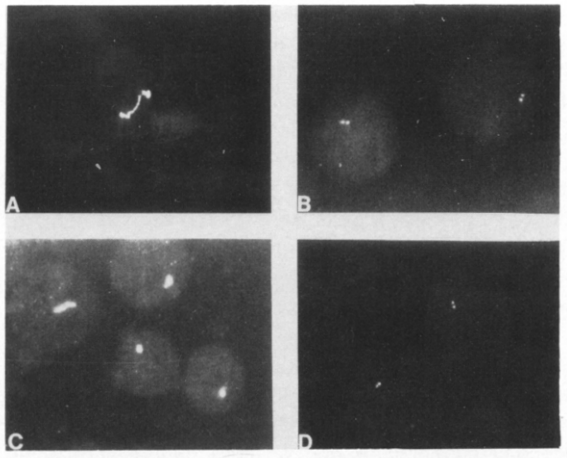

Figure 2. Fluorescent Detection of Specific RNA and DNA Sequences in Unstained Nuclei

(A) High magnification view of nuclear RNA from the BamHI W region of EBV in Namalwa cells showing intense fluorescence signals at both ends of the RNA track. 1200×.

(B)Detection of the EBV Bam W DNA in denatured nuclei treated with RNAase H after hybridization. Two closely spaced genomic signals are apparent. 800×.

(C) Detection of the EBV Bam Y/H RNA in nuclei of Namalwa cells. 650×.

(D) Detection of the EBV Bam A DNA in denatured nuclei without RNAase H treatment. Evidence of nuclear RNA is not detected, and the two genomic signals are observed only in denatured nuclei. 650×.

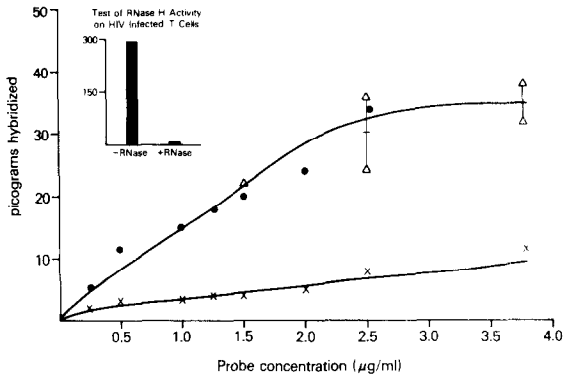

Figure 3. Quantitation of EBV BamHI Fragment W Nuclear RNA

Glass slides containing equivalent densities of Namalwa interphase nuclei were hybridized overnight, as described, with increasing concentrations of Bam W probe. Hybridization was quantitated by Cerenkov radiation in a scintillation counter. Circles and triangles indicate hybridization to samples from two experiments. After scintillation counting of samples in PBS, the same samples were treated with RNAase H as described, and samples were recounted to derive the control curve (X). The number of nuclei on each slide was estimated by microscopic counts of DAPI-stained nuclei. The average amount of probe hybridized per nucleus was calculated to estimate the equivalent number of target sequences detected (see Results).

hybridization and detection of EBV DNA alone revealed two closely paired pinpoints of fluorescence (each 0.1–0.2 μ in diameter) separated by an average 1.7 μm (range 0.3–3 μ), representing two closely integrated genomes. When parameters were adjusted to allow RNA detection as well as RNA, the tiny paired genomic signals were no longer discernible because of the much brighter and larger signal generated by the RNA. RNA "tracks" were an average 5 μm in length, up to 100 times longer than the genomic signals and extending well beyond the distance separating the two integrated viral genomes (approximately 1.7 μm). Hence, the RNA signals do not correspond to nascent transcripts being synthesized along the DNA strand (i.e., the "christmas tree;" Miller, 1981), but represent a much larger accumulation of RNA that extends well beyond the dimensions of the gene.

To calculate the average amount of RNA detected in each interphase nucleus, quantitative saturation experiments were conducted in which a ^{32}P-labeled Bam W probe was hybridized at increasing concentrations to samples containing equal densities of Namalwa interphase nuclei (see Figure 3). Hybridization was quantitated by Cerenkov radiation in a scintillation counter, and the average number of nuclei per coverslip was determined from counting of DAPI-stained nuclei in a microscope. The average amount of probe hybridized per nucleus was calculated after correction for nonspecific sticking of probe, as indicated by negative controls including RNAase-treated samples and samples reacted with labeled plasmid DNA without insert (Figure 3). In replicate experiments, the average amount of probe hybridized per nucleus was approximately 900 kb, the equivalent of roughly 300 copies of the 3 kb Bam W sequence. Nuclei with larger RNA signals may have 3- to 4-fold this amount.

The curving linear structures detected by in situ hybridization, each containing a few hundred RNA transcripts, were most commonly unbranched, but bifurcated tracks were not uncommon. The structure and general appearance of RNA tracks from many different nuclei are diagramatically represented in Figure 4B. The intensity of fluorescence along these structures was not uniform. As shown at high magnification in Figure 2A, most RNA tracks had a focal point of very intense fluorescence at one or both ends of the linear structure and frequently less intense foci along their length. These bright points do not represent detection of the EBV genome, since they are present without denaturation of nuclear DNA prior to hybridization, are more intense than the signal produced by each genome, and are usually spaced much further apart than the average 1.7 μm separating the genomes. The distant spacing of these focal points also precludes the possibility that they represent an accumulation of RNA at the site of transcription from the viral genomes. Alternatively, accumulations of RNA may occur at some point in the processing or transport path, such as, for example, a build up of transcripts at the nuclear pore.

Essentially identical tracks of specific viral RNAs were observed in other latently infected EBV cell lines, including IB-4 and Raji cells (Figure 1F). Although the IB-4 cell line contains one integrated copy of the EBV genome and several episomal copies (van Santen et al., 1983; Henderson et al., 1983) and Raji nuclei contain approximately 50

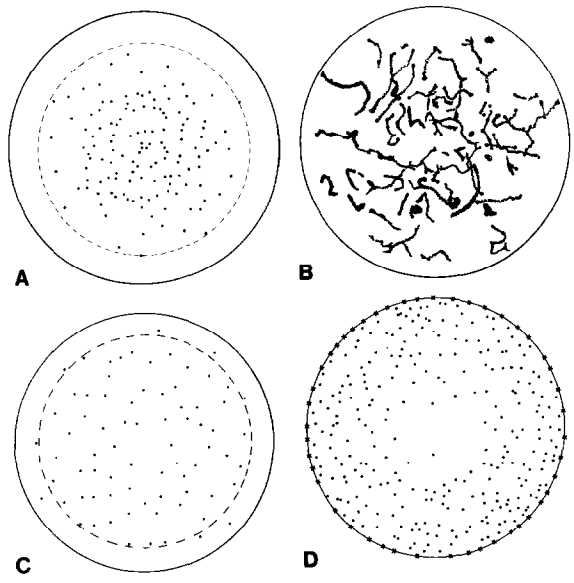

Figure 4. Distribution of EBV Genomes and Transcripts within Interphase Nuclei

All experiments used the BamHI W probe, and results presented are based on analysis of hundreds of randomly selected nuclei. Because the analysis is on freely rotated nuclei, the distribution presented provides three-dimensional information (see Results). (A) and (B) Isolated interphase nuclei of cytogenetic preparations. (C) and (D) Nuclei of paraformaldehyde-fixed intact cells.

(A) EBV genome distribution in isolated nuclei. Each spot represents the placement of the EBV genome relative to the center of the nucleus and randomized 360°C. For each nucleus, both the radius and the distance from the center to the most distal signal was measured from photographs using an automated digital planimeter. The distance from the center to each signal was expressed as a fraction of the corresponding radius, and results were plotted as shown.

(B)Composite distribution of transcript tracks within isolated nuclei. To represent the appearance and distributions of transcript "tracks" from many interphase nuclei, RNA signals were traced from projections of photographic slides enlarged to fit a standard-sized nucleus drawn on a piece of paper.

(C) EBV genome distribution in nuclei of intact cells. Signals were mapped as described in (A).

(D) Distribution of the outermost point of RNA signal in nuclei of intact cells. Signals were mapped as in (A) and (C), except for RNA rather than DNA.

episomal EBV genomes (Pritchett et al.,1976), these cells generally exhibited only one or two tracks of localized nuclear RNA, similar to Namalwa cells. Hence the occurrence of such RNA tracks is not a unique property of Namalwa cells, and singular sites of accumulated RNA are observed even in cases in which multiple genomes are present.

Detection of Primary Transcripts within the Nucleus of Intact, Paraformaldehyde-Fixed Cells

The above experiments were performed on interphase nuclei present in standard cytogenetic preparations that had been swollen in hypotonic solution, fixed in methanol:acetic acid, and dropped on glass slides to promote nuclear flattening and eliminate surrounding cytoplasm. To further investigate the distribution of primary transcripts as it relates to nuclear structure, it was necessary to adapt our techniques specifically for detection of RNA within the nuclei of morphologically preserved intact cells. The steps in the cytogenetic protocol were individually evaluated to derive a protocol for nuclei of intact cells. We found that intact cells grown in suspension could be gently adhered to glass slides (Cell-Line), directly fixed in 4% paraformaldehyde, stored in 70% EtOH, and then hybridized and detected by the same protocols used for isolated nuclei. The quality of hybridization obtained for nuclei of intact cells showed a degree of sensitivity and hybridization efficiency similar to that previously described for isolated nuclei (Lawrence et al., 1988a). Nuclear transcripts were detected in essentially all nuclei, as was 5 kb of single copy DNA in individual nuclei. Representative cells showing hybridization to nuclear RNA are shown in Figure 1G. The appearance of the nuclear RNA tracks within intact cells was similar to that of isolated nuclei, except that the tracks within the smaller intact cell nuclei (which had not been swollen in hypotonic solution) tended to be less elongated and their lengths less variable.

Position of the Transcribed Viral Genome and Its RNA Products within Interphase Nuclei

It is of interest to consider how these RNA tracks and the DNA sequences from which they are transcribed are positioned within the interphase nucleus. We could begin to address this by taking advantage of the fact that analysis of many freely rotated nuclei provides information about the depth of the sequences within the nuclear sphere, by essentially providing visualization of these sequences from all different angles. As previously described (Lawrence et al., 1988a), using this approach we found that the integrated EBV genome (on Chromosome 1) is restricted to an inner nuclear sphere defined by 0.8 r (r = radius), which represents only 51% of the nuclear volume (Figure 4A). This exclusion of the genome from the nuclear periphery demonstrates a nonrandom higher level organization to sequences within the nucleus, and also shows that transcribed genes need not be localized near the nuclear envelope (see Discussion). This restriction of sequences to the central region of the nucleus is not an artifact, since in the same preparations other single copy sequences are observed directly at the edge of the nucleus. For example, X chromosome sequences are observed on or very near the nuclear envelope in over 30% of nuclei (data not shown). Furthermore, a very similar pattern of distribution for the EBV sequences is observed in hybridization to nuclei of intact cells (see below).

Given the preferential localization of EBV to the nuclear interior, the question arose whether transcripts from these genes would also be restricted to the inner domain of the nucleus or whether, perhaps, the "tracks" of RNA extend from the gene towards the nuclear envelope. In Figure 4B, the positions and appearance of a number of RNA signals have been diagrammed, and comparison with Figure 4A shows that the viral transcripts are not excluded from the peripheral region of the nucleus, as are the viral genomes from which they are transcribed. To eliminate any distortions due to swelling and flattening of nuclei within

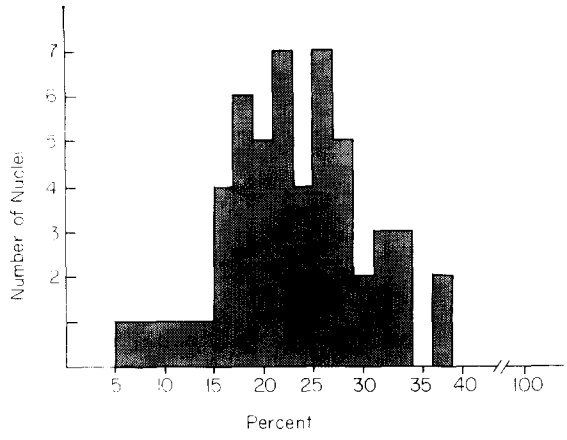

Figure 5. Length of RNA Signals in Nuclei of Intact Namalwa Cells

After hybridization with the EBV Bam W probe, the length of the RNA track and the nuclear radius for each cell was measured from photographs using a digital planimeter. Length of RNA signal is presented as a percentage of the nuclear radius for approximately 60 paraformaldehyde-fixed intact cells.

cytogenetic preparations, a similar analysis was conducted on nuclei within paraformaldehyde-fixed intact cells grown in suspension. In Figure 4C the most peripheral site of DNA signal for intact cell nuclei has been mapped as in Figure 4A, and results confirm their restriction to an inner nuclear sphere. In contrast, a very different distribution was observed for the outermost point of the RNA tracks for intact cell nuclei (Figure 4D). Comparison of Figures 4C and 4D indicated that 53% of the RNA "tracks" are observed to extend into the nuclear periphery (the region from which the gene is restricted), and 15% appear to contact the nuclear envelope directly. Hence we can conclude from Figure 4D that most, if not all, of the RNA signals extend into this peripheral region, since signals that are at the periphery will appear to be there only a fraction of the time, due to nuclear rotation. As expected, the distribution of the innermost point of RNA signal does not differ significantly from that of EBV DNA (Figure 4A compared with 4B, innermost points). These comparisons of RNA and DNA distributions provide evidence that the integrated EBV genome resides in the central region of the nucleus, and that large accumulations of highly localized RNA form a structure that extends from this region into the nuclear periphery.

Further support for this interpretation derives from the observed lengths of transcript tracks compared with the length that might be predicted from the gene distribution within interphase nuclei. In analysis of randomly rotated nuclei, the most likely site of localization for a sequence is at the interface between the inner sphere in which signal is observed and the outer sphere from which it is absent. Hence, in Namalwa cells, the most likely fixed or preferred position for the EBV genome is at approximately 0.8r (Figures 4A and 4C), and, if so, transcript tracks extending from the gene to the nuclear envelope would be expected to be approximately 0.2r in length. The histogram in Figure 5 shows that transcript tracks clearly clustered around this length, with an average of 0.228r ± 0.0263. These results are consistent with the suggestion that "tracks" of RNA extend from the gene toward the nuclear envelope.

Related to these results are observations from experiments in which cells were treated with actinomycin D to inhibit transcription prior to fixation. The amount of RNA signal decreases progressively with length of treatment in actinomycin D, such that substantial RNA signals are still detected in cells treated for 1 hr, and a 5 hr treatment is necessary to eliminate nuclear RNA. Since inhibition of transcription by actinomycin D is rapid (Singer and Penman, 1973), this progressive decline in RNA signal can be presumed to reflect the gradual loss of nuclear RNAs that were made prior to drug treatment. From the distribution of the small residual RNA signals in samples treated for 3 hr in actinomycin D (illustrated in Figure 1E), it is apparent that the remaining RNA, presumably synthesized prior to drug treatment, is not near the nuclear periphery but has a central distribution similar to that of the EBV genome (Figure 4A). In fact, simultaneous hybridization to DNA as well as residual RNA on denatured, actinomycin-treated slides indicates that these two signals must be coincident since they could not be visualized as separate in several experiments. Therefore, the movement of newly synthesized RNA toward the nuclear envelope is apparently halted by inhibition of RNA synthesis with actinomycin D. These results suggest a coupling of the viral nuclear RNA transport to transcription, which will be further investigated.

Detection of a Nonviral Nuclear RNA Abundantly Expressed in the Cytoplasm

In the above experiments, the detection of EBV nuclear RNA may have been facilitated by the accumulation of these RNAs within the nucleus of latently infected cells. Because the mature 3 kb mRNA molecules are smaller than nuclear RNA and little is transported to the cytoplasm (approximately 3 molecules of LT-1 per cell; van Santen et al., 1983; Dambaugh et al., 1986), essentially no RNA is detected in the cytoplasm of intact Namalwa cells with either the Bam W, Bam K, or Bam Y/H probes. It was of interest to determine whether a nuclear signal could be detected for a nonviral RNA that was expressed at high levels in the cytoplasm. Intact 3T3 cells stably transfected with a plasmid containing human *neu* oncogene cDNA (erb B2) provided a convenient nonviral test system, since these cells overexpress this sequence and the 4.6 kb mature mRNA is large enough to detect readily by fluorescence microscopy (see Discussion). As shown in Figure 1H, both nuclear and cytoplasmic *neu* oncogene RNA was successfully detected in the transfected cells. The nuclear signals can still be visualized, despite the diffuse cytoplasmic fluorescence. Most cells contained a single site of concentrated nuclear RNA, although occasional cells contained several nuclear foci and others none. Because of the more three-dimensional nature of these cells, the nuclear signal was not in focus in all cells (Figure 1H); however, there was an excellent correlation between the presence of cytoplasmic RNA and the presence of foci of

nuclear RNA. Cytoplasmic RNA was apparent as a diffuse punctate staining throughout the cytoplasm, frequently with brighter fluorescence in the thicker perinuclear region (Figure 1H). That this represented bona fide detection of *neu* RNA was indicated not only by the correlation between cytoplasmic and nuclear label, but by the absence of all signal in nontransfected control samples or cells hybridized with nonhomologous probe (data not shown). These results show that the ability to detect nuclear RNAs is not exclusive to the latent viral infection and that a highly localized concentration of a specific RNA is observed within nuclei of cells that are transporting this RNA to the cytoplasm in high abundance. The focus or "track" of nuclear RNA was not as extended as frequently observed for the viral RNA of intact cell nuclei (Figure 1G), but was often slightly elongated and clearly represents localization of many transcripts, as evident from comparison with the fine punctate fluorescence indicative of *neu* mRNA molecules throughout the cytoplasm.

Discussion

This work demonstrates high-resolution visualization of the distribution of specific transcribed nuclear RNAs directly within interphase nuclei. Fluorescent detection of nonisotopic in situ hybridization revealed a striking localization of viral RNAs within nuclei of latently infected lymphoma cells. Several hundred copies of specific RNA sequences are tightly restricted to a small region of the nucleus, often in a curvilinear "track". All of the specific RNA detected is confined within the distinct boundaries of the track or focus, with no evidence of a diffuse distribution or gradient throughout the nucleus. The dimensions of the RNA signals (up to several microns in length) are far greater than those of the corresponding DNA signals (0.1–0.2 μm). Therefore, the accumulation of nuclear RNA extends well beyond the locale of the gene and is not the "christmas tree" of nascent transcripts observed along the loops of lampbrush chromosomes by electron microscopy, which represents a higher magnification view of a much smaller area (Miller, 1981). Several lines of evidence confirmed that these results represent genuine detection of specific nuclear transcripts: hybridization in the absence of denaturation, sensitivity to RNAase H or RNAase A, sensitivity to actinomycin D, and correlation with known transcribed sequences of the EBV genome. The significance of these results for the general study of gene expression and their immediate relevance for understanding nuclear RNA transport and metabolism as it relates to nuclear structure are discussed below.

The nature of the specific RNA distributions observed provides fundamental insights into the basic structure of the nucleus and the general mechanism of RNA transport. The precise localization of specific nuclear RNAs argues strongly against free diffusion of RNA through the nucleoplasm, but is much more consistent with a solid-phase model of nuclear structure in which RNA molecules are actively transported from their site of synthesis to the nuclear pores. The appearance of a track of nuclear transcripts provides direct evidence that transcripts from specific genes are transported vectorially toward a single or small subset of nuclear pores. In general, our results advance a view of nuclear structure based upon a nonrandom organization of genes and their transcripts within interphase nuclei. While this is consistent with aspects of a hypothesis previously described by Blobel (1985) as "gene gating", these results do not address a keypoint of this hypothesis that proposes that nuclear pores organize and are attached to transcribed genes. The demonstration that the expressed EBV genome resides in an inner nuclear sphere clearly indicates that DNA sequences need not be adjacent to the nuclear envelope to be transcribed, although "channels" of active chromatin that enter the nuclear interior may exist (see Hutchinson and Weintraub, 1985). Findings from other laboratories have shown a diffuse localization throughout the nuclear periphery of RNA polymerase II (Clark and Hamkalo, 1987) and RNA11, a protein component of the yeast splicing apparatus (Chang et al., 1988).

The often linear structure formed by the accumulated transcripts is suggestive of a fibrillar attachment, providing indirect evidence for a nuclear matrix to which hnRNA is bound. This evidence corroborates a body of work on nuclear structure derived from an entirely different approach using biochemical fractionation of cells (see Introduction). In results presented here, it is unlikely that RNA is confined to a precise position by compression between other nuclear material (i.e., chromatin) for several reasons. If the RNA were simply confined to a space within the nucleus, hypotonic swelling and acid fixation would be expected to disrupt or diffuse its localization. On the contrary, these treatments render the specific nuclear RNA distribution even more defined and linear, presumably by distending internal nuclear structures with which the RNA is associated. The morphological preservation of the hnRNA throughout these procedures, known to release cytoplasmic RNA (Lawrence and Singer, 1985), may be effected by tight binding to nuclear structures, as well as being bound by ribonuclear proteins. Finally, preliminary experiments show that removal of nuclear components by triton and DNAase treatment prior to paraformaldehyde fixation does not affect the track of nuclear RNA (unpublished data).

The nuclear RNA visualized may be in an RNA processing compartment and/or transport path. The fact that a diffuse distribution of RNA is not detected near the "track" or anywhere within the nucleus indicates that RNAs are not free to diffuse during either processing or transport, although it is possible that small quantities of fully processed RNA escape detection. Analysis of the relative 3-D distributions of RNA and DNA indicate that the RNA extends into a markedly more peripheral position than does the genome from which it is transcribed, consistent with the extension of an RNA path toward the nuclear envelope. These results cannot be explained simply by the greater length of RNA versus DNA signals, since the innermost point of RNA signal shows a distribution similar to that of the genome. This type of analysis allowed us to overview the general pattern of distribution from many cells; however, optical sectioning using confocal micros-

copy is currently being pursued in order to characterize more precisely, for individual nuclei, the position of RNA with respect to the nuclear envelope and nuclear pores.

A localized export of a particular RNA from the nucleus could result in, or contribute to, an asymmetric mRNA distribution within the cytoplasm, potentially an important component in establishment of cell morphology and polarity or, possibly, in the determination of developmental fate. Under the hybridization conditions used in these experiments, the *neu* mRNA in transfected 3T3 cells (Figure 1H) does not appear to be concentrated in a particular region of the cytoplasm, despite focal concentrations within the nucleus. However, we have previously demonstrated the existence of distinct distributions of specific cytoplasmic mRNAs in somatic cells, particularly mRNAs for different cytoskeletal proteins and for histones (Lawrence and Singer, 1986; Lawrence et al., 1988b). Other investigators have described nonrandom distributions of specific mRNAs within oocytes (Jeffrey et al., 1983; Jeffrey, 1984; Weeks and Melton, 1987). Taken together, the distinct and nonrandom distributions of cytoplasmic mRNAs observed, coupled with the precise localization of nuclear RNA reported here, support the concept that RNAs are specifically organized within cells and may be physically associated with the solid-state cellular architecture from transcription through translation.

It is apparent from our results that for three different cell types latently infected with EBV, there is an abundance of certain RNA sequences within the nucleus relative to the cytoplasm. Similar distributions of viral nuclear RNA were observed in three different EBV-infected cell lines, regardless of the number of viral genomes carried, and in nuclei fixed by two entirely different methods, including nuclei within paraformaldehyde-fixed, morphologically intact cells. We have also observed intense nuclear RNA signals in other cells productively infected with HIV or EBV (unpublished data). Results with the *neu* oncogene–transfected 3T3 cells were included to show that the localized concentration of nuclear RNA is not specific to viral infection. The fact that the nuclear RNA "tracks" in this case are not as elongated as they were for the viral nuclear RNAs may be related to the more extensive processing (e.g., splicing) that the viral RNAs undergo, or to integration of the EBV genome in a more internal nuclear site, or, conceivably to some property common to different latently infected cells that results in a build up of RNA along the processing or transport path. By disrupting endogenous nuclear metabolism at different steps, as in the preliminary actinomycin experiments reported here, it may be possible to decipher the relationship among processing, transport, and nuclear structure. Unlike in vitro RNA efflux methods, direct visualization by in situ hybridization provides a method of investigating RNA transport across the nucleoplasm distinct from translocation across the nuclear pore.

A major significance of this work is that the ability to detect transcripts near their site of synthesis is a potentially powerful tool for the general study of gene expression and regulation. This methodology provides an assay for newly synthesized RNA directly within individual cells, in contrast with other in situ hybridization techniques that detect the presence of accumulated mRNAs, but cannot distinguish ongoing or recently initiated gene activity. Currently applications of this approach are most likely to be successful for larger abundant RNAs that are well represented in the cell nucleus, particularly those that undergo extensive processing. While small, unprocessed histone mRNAs were not detected, we have recently detected nuclear transcripts from the neurotensin gene in induced PC12 cells (unpublished data). The ability to detect RNAs by fluorescence in either the nucleus or the cytoplasm depends not only upon their abundance, but also upon their distribution and the size of the original target molecules. Currently molecules smaller than a few kb are not easily visible by a one-step fluorescein-avidin detection without the use of amplification procedures, which tend to enhance background (Lawrence et al., 1988a). For this reason, we have continued to use autoradiography for detection and localization of most cytoplasmic mRNAs (Lawrence and Singer, 1986; Lawrence et al.,1988b) or, in some cases, enzymatic detection techniques (Singer et al., 1986; Lawrence and Singer, 1986), both of which allow signal amplification by increased exposure or reaction times.

The continued development and application, in a number of laboratories, of in situ hybridization techniques providing high resolution, sensitivity, and morphological preservation advances an approach to cellular organization and gene expression appropriately termed "molecular cytology." It should be possible to investigate gene expression from this perspective as a continuum, from the potential cell type–specific localization of sequences within the nucleus (Manuelidis, 1984), to the synthesis, processing, and transport of nuclear RNA, and ultimately, to the localization and translation of the mRNA within the cytoplasm.

Experimental Procedures

The methodology described here is based upon previously developed methods for fluorescence detection of single-copy DNA sequences (Lawrence et al., 1988a) that have been optimized and modified for detection of RNA. This approach utilizes biotin labeling of DNA (Langer et al., 1981; Langer-Safer et al., 1982) and a straightforward one step detection method with fluorescein-avidin, which in our hands gives lower background, higher resolution, and better reproducibility than antibodies to biotin. This methodology has been reproducible with 90% success for over a year in our laboratory, with the exception of a period of two months during which nuclear RNA was degraded for unknown reasons, presumably related to quality control of key reagents. In general, autoclaving of solutions and inclusion of an RNAase inhibitor during hybridization are sufficient to prevent RNA loss during processing.

Cell Culture and Nuclear Preparations

The Namalwa and IB-4 cell lines (obtained from Elliot Kieff) were maintained in suspension in RPMI medium with 10% fetal calf serum (Gibco, NY), as were Raji cells (obtained from John Sullivan). For analysis of interphase nuclei and metaphase chromosomes, standard cytogenetic preparations were made after incubation of cells at 37°C with 0.015 μg/ml of colcemid (demicolcine) for 2–3 hr. Cells were then harvested and incubated in 0.075 M KCl at 37°C for 17 min. The cell suspension was fixed in three changes of 3:1 methanol:acetic acid and dropped onto glass slides. Slides were air-dried overnight and stored at −80°C with dessicant. In some experiments, the colcemid treatment was omitted without significantly affecting results on interphase nuclei.

For inhibition of transcription, cells were incubated in 4 μg/ml of actinomycin D for 5 hr prior to fixation.

For hybridization to nuclei of intact lymphoma cells, suspension cells in phosphate buffered saline (PBS) were placed at high density onto Cell-Line multiwell slides and allowed to adhere briefly until almost dry. Cell samples were then fixed in 4% paraformaldehyde in PBS for 5 min and stored at 4°C in 70% EtOH for further use. The mouse 3T3 cell line stably transfected with the *neu* oncogene cDNA in a mammalian expression vector (pMAX) was the gift of Applied Biotechnology (Cambridge, MA) and was grown in DMEM, 10% FCS, and 300 μg/ml of neomycin (G418). These monolayer cells were grown on glass coverslips and fixed in paraformaldehyde as described for intact Namalwa cells.

Probes and Nick Translation

The EBV probes were provided by Jim Skare and represent the BamHI W, Y/H, A, and K fragments of the genome in a pBR322 vector (Skare and Strominger, 1980; Lawrence et al., 1988a). The BamHI W and Y/H sequences are transcribed in a leftward direction, beginning in U1 or IR2, into a primary transcript as large as 20 kb. These are extensively spliced into the 3 kb LT-1 polyadenylated mRNA, which contains a total of 0.9 kb of Bam W sequences and 1.9 kb of Y/H sequences (van Santen et al., 1983). Small exons from the BamHI W and Y/H region of EBV can be alternatively spliced with other rightward sequences to form very low abundance mRNAs coding for nuclear antigens (Austin et al., 1988). The *neu* oncogene probe was a 4.6 kb cDNA clone provided by Applied Biotechnology. Plasmid DNA was nick-translated by established procedures using biotinated-11-dUTP (BRL or Enzo Biochemical, NY) and unincorporated nucleotides removed using Sephadex G50 columns. DNAase concentrations were adjusted so that probe fragment size after nick translation was 200–800 nucleotides. Probe size and biotin incorporation were monitored by alkaline agarose gel electrophoresis, transfer to nitrocellulose filter, and visualization using streptavidin and biotinylated alkaline phosphatase (BRL, Gaithersburg, MD).

Hybridization

Nuclear preparations were incubated for 10 min in 0.1 M triethanolamine and 0.25% acetic anhydride. For hybridization to DNA sequences, samples were denatured at 70°C for 2 min in 70% formamide, 2× SSC. This step was omitted for hybridization to RNA exclusively, as it tended to weaken RNA signals to some degree. Preparations were dehydrated through cold 70%, 95%, and 100% EtOH for 5 min each and air-dried. For each sample, 50 ng of probe, 5 μg of sonicated salmon sperm DNA, and 20 μg of E. coli tRNA were suspended in 5 μl of deionized formamide and heated at 70°C–80°C for 10 min. An equal volume of hybridization buffer was added, so that the final hybridization solution contained 50% formamide, 2× SSC (0.3 M sodium citrate), 1% BSA, 10% dextran sulfate, and 10% vanadyl sulfate. The hybridization solution was placed on samples, covered with parafilm, and incubated at 37°C in a humidified chamber overnight. Rinses were for 30 min each in 50% formamide. 2× SSC at 37°C, 2× SSC, and finally 1× SSC at room temperature. For RNAase treatment, samples were treated after hybridization with RNAase H used at 8 U/ml for 1–2 hr at 37°C in a buffer consisting of 100 mM KCl, 20 mM Tris–HCl (pH 7.5), 1.5 mM $MgCl_2$, 50 μg/ml of BSA, 1 mM DTT, 0.7 mM EDTA, and 13 mM HEPES (Minshull and Hunt, 1986). For elimination of RNA, RNAase A could also be used prior to hybridization at 100 μg/ml in 2× SSC for 1 hr.

Detection and Nuclear Stain

Hybridization was detected using avidin conjugated to fluorescein (Enzo Biochemical, NY). Samples were incubated in 2 μg/ml of avidin in 4× SSC, 1% BSA for 30 min at room temperature. Samples were then rinsed at room temperature for 10 min each in 4× SSC, 4× SSC with 0.1% triton, and then 4× SSC. For visualization of total DNA, samples were stained with either DAPI (diaminophenylindole) for 5 min in PBS or propidium iodide for 1 min at 0.5 μg/ml in PBS. Samples were mounted in antibleach mounting medium (Johnson and Aroujo Nogueria, 1981) and stored in the dark at 4°C.

Microscopy

Samples were visualized at 1000× magnification using a 100× neofluor objective on a Zeiss ICM microscope equipped with epifluorescence filters. Black and white photographs were taken on Tri-X (ASA 400 film), and color photographs on Ektachrome 400. Exposure times were 1–2 min. No image-processing devices were utilized.

Acknowledgments

We would especially like to acknowledge the excellent technical contribution of Carol Villnave Johnson during the early phase of this work. We thank Marie Georgio for her expertise in color photographic processing and Adam Singer for his assistance with this. We appreciate the technical assistance of John McNeil, the administrative assistance of Elayn Byron, and the gift of the *neu* oncogene–transfected 3T3 cells from Applied Biotechnology. We thank Ted Fey for thoughtful reading of the manuscript. This work was supported by grant HD18066 from the National Institute of Health to R. H. S., and J. B. L. and a Muscular Dystrophy Association Grant to J. B. L.

The costs of publication of this article were defrayed in part by the payment of page charges. This article must therefore be hereby marked "*advertisement*" in accordance with 18 U.S.C. Section 1734 solely to indicate this fact.

Received September 23, 1988; revised February 24, 1989.

References

Agutter, P. S. (1985). RNA processing, RNA transport and nuclear structure. In Nuclear Envelope Structure and RNA Maturation (New York: Alan R. Liss), pp. 539–559.

Austin, P. J., Flemington, E., Yandava, C. N., Strominger, J. L., and Speck, S. H. (1988). Complex transcription of the Epstein–Barr virus Bam HI fragment H rightward open reading frame 1 (BHFR1) in latently and lytically infected B lymphocytes. Proc. Natl. Acad. Sci. USA *85*, 3678–3682.

Berezney, R. (1980). Fractionation of the nuclear matrix. J. Cell Biol. *85*, 641–650.

Berezney, R., and Coffey, D. S. (1974). Identification of a nuclear protein matrix. Biochem. Biophys. Res. Commun. *60*, 1410–1419.

Beyer, A. L., Christensen, M. E., Walker, B. W., and Le Stourgeon, W. M. (1977). Identification and characterization of the packaging proteins of core 40S hnRNP particles. Cell *11*, 127–138.

Blobel, G. (1985). Gene gating: a hypothesis. Proc. Natl. Acad. Sci. USA *82*, 8527–8529.

Borun, T. W., Scharff, M. D., and Robbins, E. (1967). Rapidly labelled, polyribosomes-associated RNA having the properties of histone messenger. Proc. Natl. Acad. Sci. USA *58*, 1977–1983.

Brasch, K. (1982). Fine structure and localization of nuclear matrix *in situ*. Exp. Cell Res. *140*, 161–171.

Capco, D., and Penman, S. (1983). Mitotic architecture of the cell: the filament networks of the nucleus and cytoplasm. J. Cell Biol. *96*, 896–906.

Chang, T.-H., Clark, M. W., Lustig, A. J., Cusick, M. E., and Abelson, J. (1988). RNA11 protein is associated with the yeast spliceosome and is localized in the periphery of the cell nucleus. Mol. Cell. Biol. *8*, 2379–2393.

Clark, R. F., and Hamkalo, B. A. (1987). Localization of nuclear proteins by immunogold staining and electron microscopy. J. Cell Biol. *105*, 71a.

Clawson, G. A., Feldherr, C. M., and Smuckler, E. A. (1985). Nucleocytoplasmic RNA transport. Mol. Cell. Biochem. *67*, 87–99.

Dambaugh, T. K., Hennessey, K., Fennewald, S., and Kieff, E. (1986). The virus genome and its expression in latent infection. In the Epstein–Barr Virus: Recent Advances, M. A. Epstein and B. G. Achong, eds. (New York: John Wiley and Sons), pp. 13–45.

Fey, E. G., Krochmalnic, G., and Penman, S. (1986). The non-chromatin substructures of the nucleus: the ribonucleoprotein (RNP)-containing and RNP-depleted matrices analyzed by sequential fractionation and resinless section electron microscopy. J. Cell Biol. *102*, 1654–1665.

Fey, E. G., Wan, K. M., and Penman, S. (1984). Epithelial cytoskeletal framework and nuclear matrix-intermediate filament scaffold: three-

dimensional organizational and protein composition. J. Cell Biol. *98*, 1973–1984.

Georgiev, G. P., and Chentsov, Y. S. (1960). Epstein–Barr virus specific RNA I. On the structure of cell nucleus. Experimental electron microscopic studies on the isolated nuclei. Proc. Natl. Acad. Sci. USSR *132*, 199–201.

Hayward, S., and Kieff, E. (1976). Epstein–Barr virus specific RNA I. Analysis of viral RNA in cellular extracts and in the polyribosomal fraction of permissive and nonpermissive lymphoblastoid cell lines. J. Virol. *18*, 518–525.

Heller, M., Dambaugh, T., and Kieff, E. (1981). Epstein–Barr virus DNA. IX. Variation among viral DNAs. J. Virol. *38*, 632–648.

Henderson, A., Ripley, S., Heller, M., and Kieff, E. (1983). Chromosome site for Epstein–Barr virus DNA in a Burkitt tumor cell line and in lymphocytes growth transformed in vitro. Proc. Natl. Acad. Sci. USA *80*, 1987–1991.

Herman, R., Weymouth, L., and Penman, S. (1978). Heterogeneous nuclear RNA–protein fibers in chromatin-depleted nuclei. J. Cell Biol. *78*, 663–674.

Hochstrasser, M., and Sedat, J. W. (1987). Three-dimensional organization of Drosophila melanogaster interphase nuclei. I. Tissue specific aspects of polytene nuclear architecture. J. Cell Biol. *104*, 1455–1470.

Hutchison, N., and Weintraub, H. (1985). Localization of DNAase I-sensitive sequences to specific regions of interphase nuclei. Cell *43*, 471–482.

Jackson, D. A., McCready, S. J., and Cook, P. R. (1981). RNA is synthesized at the nuclear cage. Nature *292*, 552–555.

Jeffrey, W. R. (1984). Spatial distribution of messenger RNA in the cytoskeletal framework of Ascidian eggs. Dev. Biol. *103*, 482–492.

Jeffrey, W. R., Tomlinson, C. R., and Brodeur, R. D. (1983). Localization of actin mRNA in during early Ascidian development. Dev. Biol. *99*, 408–417.

Johnson, G. D., and Aroujo Nogueira, G. M. (1981). A simple method of reducing the fading of immunofluorescence during microscopy. J. Immunol. Meth. *43*, 349–350.

Kawai, Y., Nonoyama, M., and Pagano, J. (1973). Reassociation kinetics for EBV DNA. Non-homology to mammalian DNA and homology to viral DNA in various diseases. J. Virol. *12*, 1006–1012.

King, W., Thomas-Powell, A. L., Raab-Traub, N., Hawke, M., and Kieff, E. (1980). Epstein–Barr virus RNA. V. Viral RNA in a restringently infected, growth transformed cell. J. Virol. *36*, 506–518.

Langer, P. R., Waldrop, A. A., and Ward, D. C. (1981). Enzymatic synthesis of biotin-labeled polynucleotides: novel nucleic acid affinity probes. Proc. Natl. Acad. Sci. USA *78*, 6633–6637.

Langer-Safer, P. R., Levine, M., and Ward, D. C. (1982). Immunological method for mapping genes on Drosophila polytene chromosomes. Proc. Natl. Acad. Sci. USA *79*, 4381–4385.

Lawrence, J. B., and Singer, R. H. (1985). Quantitative analysis of *in situ* hybridization methods for detection of actin gene expression. Nucl. Acids. Res. *13*, 1777–1799.

Lawrence, J. B., and Singer, R. H. (1986). Intracellular localization of messenger RNAs for cytoskeletal proteins. Cell *45*, 407–415.

Lawrence, J. B., Villnave, C. A., and Singer, R. H. (1988a). Sensitive, high-resolution chromatin and chromosome mapping in situ: presence and orientation of two closely integrated copies of EBV in a lymphoma line. Cell *52*, 51–61.

Lawrence, J. B., Singer, R. H., Villnave, C. A., Stein, J. L., and Stein, G. S. (1988b). Intracellular distribution of histone mRNAs in human fibroblasts studied *in situ* hybridization. Proc. Natl. Acad. Sci. USA *85*, 463–467.

Lerner, M. R., Boyle, J. A., Mount, S., Wolin, S. L., and Steitz, J. A. (1980). Are snRNPs involved in splicing? Nature *283*, 220–224.

Long, B. H., Huang, C.-Y., and Pogo, A. O. (1979). Isolation and characterization of the nuclear matrix in friend erythroleukemia cells: chromatin and hnRNA interactions with nuclear matrix. Cell *18*, 1079–1090.

Manuelidis, L. (1984). Different central nervous system cell types display distinct and non-random arrangements of satellite DNA sequences. Proc. Natl. Acad. Sci. USA *81*, 3123–3127.

Miller, O. L. (1981). The nucleolus, chromosomes and visualization of genetic activity. J. Cell Biol. *91*, 15S–27S.

Minshull, J., and Hunt, T. (1986). The use of the single-stranded DNA and RNAase H to promote hybrid arrest of translation of mRNA/DNA hybrids in reticulocyte lysate cell-free translations. Nucl. Acids. Res. *14*, 6433–6451.

Pederson, T. (1974). Proteins associated with heterogeneous nuclear RNA in eukaryotic cells. J. Mol. Biol. *83*, 163–184.

Pederson, T., and Davis, N. G. (1980). Messenger RNA processing and nuclear structure: isolation of nuclear ribonucleoprotein particles containing β-globin messenger RNA precursors. J. Cell Biol. *87*, 47–54.

Powell, A., King, W., and Kieff, E. (1979). Epstein–Barr virus specific RNA. III. Mapping of the DNA encoding viral specific RNA in restringently infected cells. J. Virol. *29*, 261–274.

Pritchett, R., Pedersen, M., and Kieff, E. (1976). Complexity of EBV homologous DNA in continuous lyphoblastoid cell lines. Virology *74*, 227–231.

Ross, D. A., Yen, R. W., and Chae, C. B. (1982). Association of globin ribonucleic acid and its precursor with the chicken erythroblast nuclear matrix. Biochemistry *21*, 764–771.

Schroder, H. C., Bachman, M., Diehl-Siefert, B., and Muller, W. (1987). Transport of mRNA from nucleus to cytoplasm. Prog. Nucl. Acids Res. *34*, 89–142.

Sharp, P. A. (1987). Splicing of messenger RNA precursors. Science *235*, 766–771.

Singer, R. H., and Penman, S. (1973). Messenger RNA in HeLa cells: kinetics of formation and decay. J. Mol. Biol. *78*, 321–333.

Singer, R. H., Lawrence, J. B., and Villnave, C. (1986). Optimization of *in situ* hybridization using isotopic and nonisotopic detection methods. Biotechniques *4*, 230–250.

Skare, J., and Strominger, J. (1980). Cloning and mapping of BamH1 endonuclease fragments of DNA from the transforming B95-8 strain of Epstein–Barr virus. Proc. Natl. Acad. Sci. USA *77*, 3860–3864.

van Eekelen, C. A. G., and van Venrooij, W. J. (1981). HnRNA and its attachment to a nuclear protein matrix. J. Cell Biol. *88*, 554–563.

Van Santen, V., Cheung, A., and Kieff, E. (1983). Epstein–Barr virus RNA. VII. Size and direction of transcription of virus-specific cytoplasmic RNAs in a transformed cell line. Proc. Natl. Acad. Sci. USA *78*, 1930–1934.

Weeks, D. L., and Melton, D. A. (1987). A maternal mRNA localized to the vegetal hemisphere in Xenopus eggs codes for a growth factor related to TGF-β. Cell *51*, 861–867.